Supplementary Information for

Sulfur and Phosphorus Co-doping of Nickel-Cobalt Layered Double Hydroxides for Enhancing Electrochemical Reactivity and Supercapacitor Performance

Kyung Su Kim[a], Nanasaheb M. Shinde[b], Je Moon Yun[b,c,*], and Kwang Ho Kim[a,b,*]

[a]School of Materials Science and Engineering, Pusan National University, San 30 Jangjeon-dong, Geumjeong-gu, Busan 609-735, Republic of Korea.

[b]Global Frontier R&D Center for Hybrid Interface Materials, Pusan National University, San 30 Jangjeon-dong, Geumjeong-gu, Busan 609-735, Republic of Korea.

[c]Division of Advanced Materials Engineering, Dong-Eui University, 176 Eomgwang-ro, Busanjin-gu, Busan, 47340, Republic of Korea.

*Corresponding author.

E-mail addresses: jmyun@deu.ac.kr (J.M.Yun), kwhokim@pusan.ac.kr (K.H.Kim)

Results and discussion

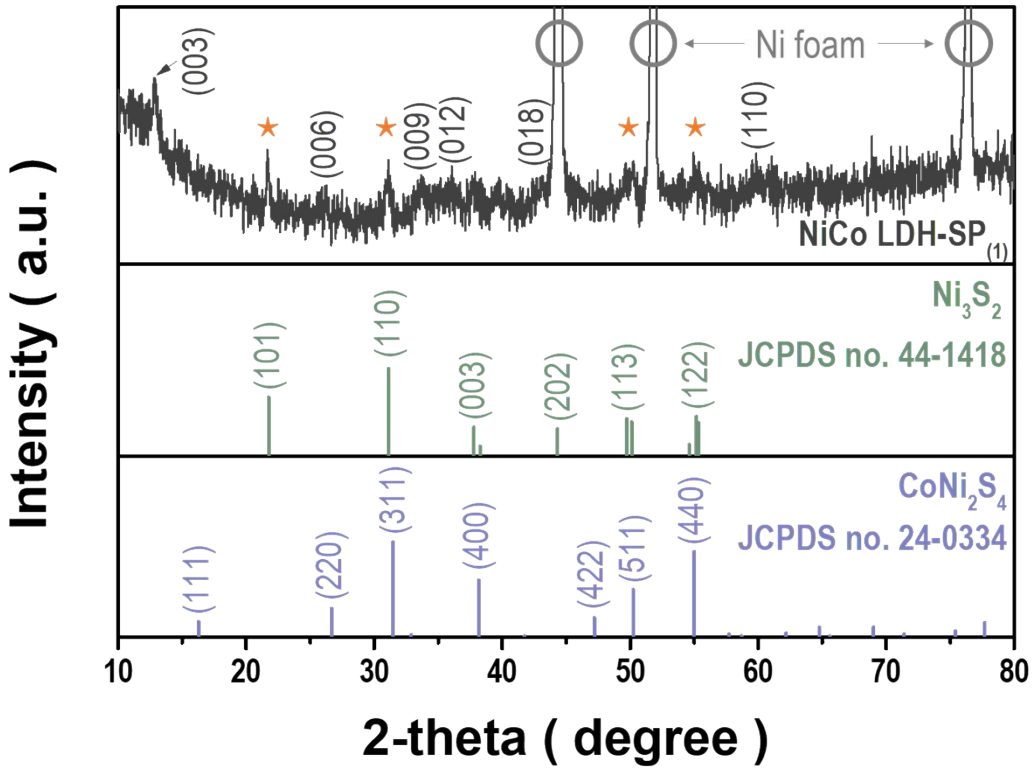

Fig. S1. XRD patterns of the NiCo LDH-$SP_{(1)}$.

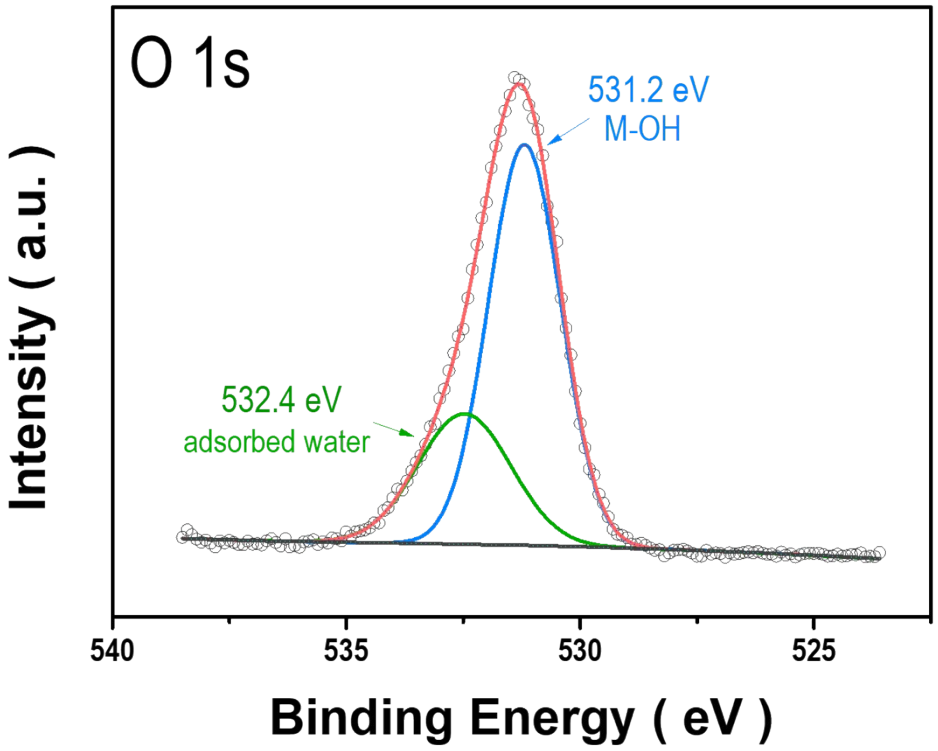

Fig. S2. High-resolution O 1s XPS spectra of the NiCo LDH-$SP_{(1)}$.

Table S1. The quantative analysis of NiCo LDH-$SP_{(1)}$.

Element	Ni	Co	O	P	S
Atomic %	18.95	6.65	70.64	1.17	2.59

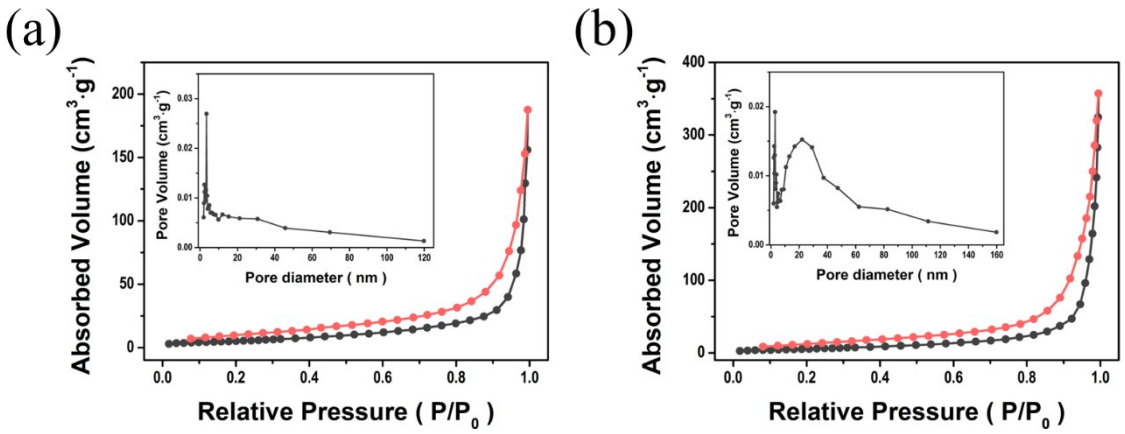

Fig. S3. Nitrogen adsorption-desorption analysis and Pore size distribution of (a) NiCo LDH and (b) NiCo LDH-$SP_{(1)}$.

Table S2. Specific surface area, pore size and pore volume of the NiCo LDH and NiCo LDH-$SP_{(1)}$.

Sample	S_{bet} (m^2 g^{-1})	d_{pore} (nm)	V_{pore} (cm^3 g^{-1})
NiCo LDH	18.52	6.72	0.242
NiCo LDH-$SP_{(1)}$	20.29	11.01	0.509

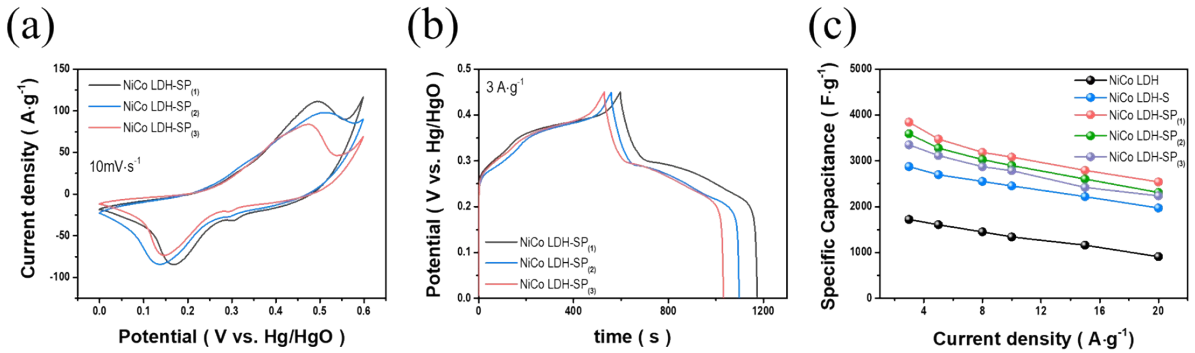

Fig. S4. Comparisons of electrochemical performances. (a) CV curves at 10 mV s^{-1}; (b) GCD curves at 3 A g^{-1} for NiCo LDH-$SP_{(1)}$, NiCo LDH-$SP_{(2)}$, and NiCo LDH-$SP_{(3)}$; (c) specific capacitance (different current densities) of all electrodes.

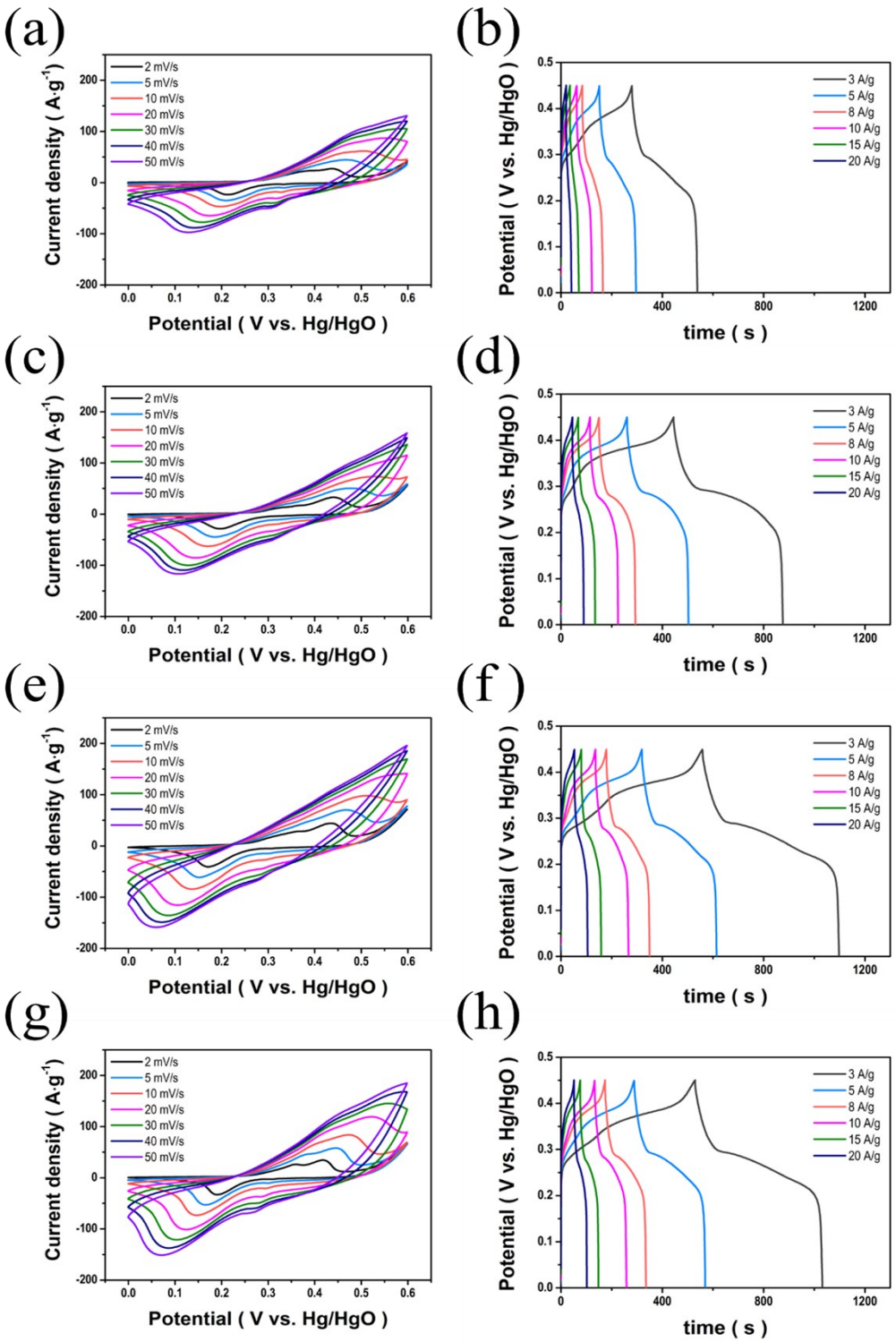

Fig. S5. CV curves at various scan rates and GCD curves at various current densities of (a-b) NiCo LDH; (c-d) NiCo LDH-S; (e-f) NiCo LDH-$SP_{(2)}$; and (g-h) NiCo LDH-$SP_{(3)}$, respectively.

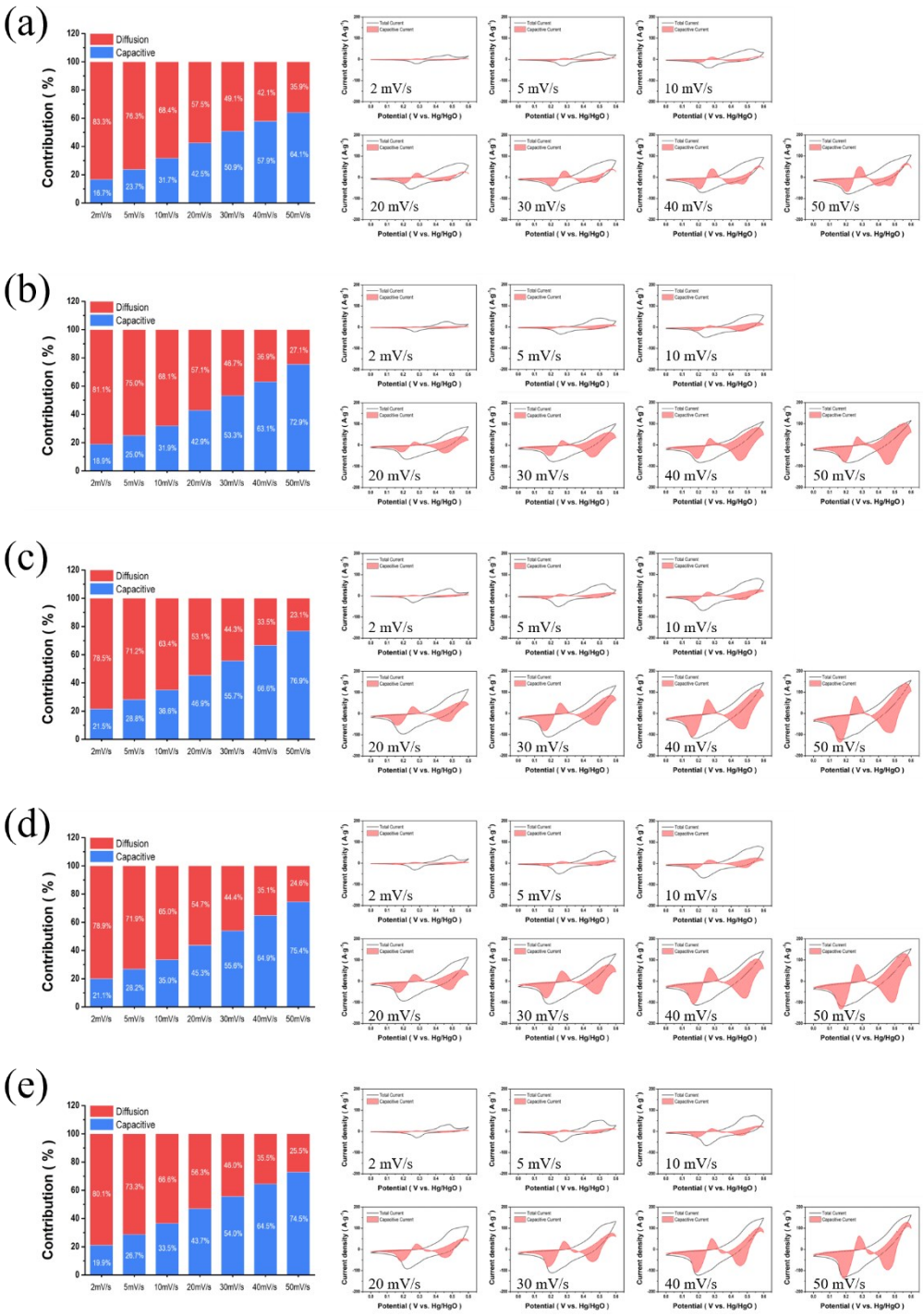

Fig. S6. Capacitive (red) and diffusion-controlled (white) contribution at 2, 5, 10, 20, 30, 40 and 50 mV s^{-1} of (a) NiCo LDH; (b) NiCo LDH-S; (c) NiCo LDH-$SP_{(1)}$; (d) NiCo LDH-$SP_{(2)}$; and (e) NiCo LDH-$SP_{(3)}$, respectively.

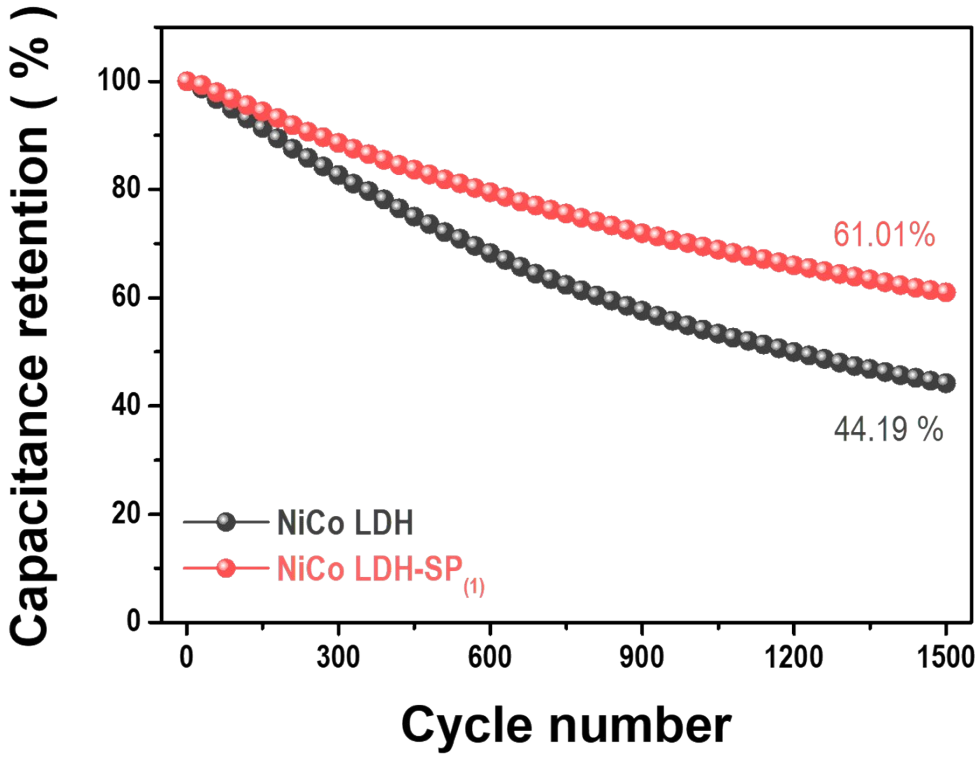

Fig. S7. Cycling stability of NiCo LDH and NiCo LDH-$SP_{(1)}$ at a current density of 20 A g^{-1}.

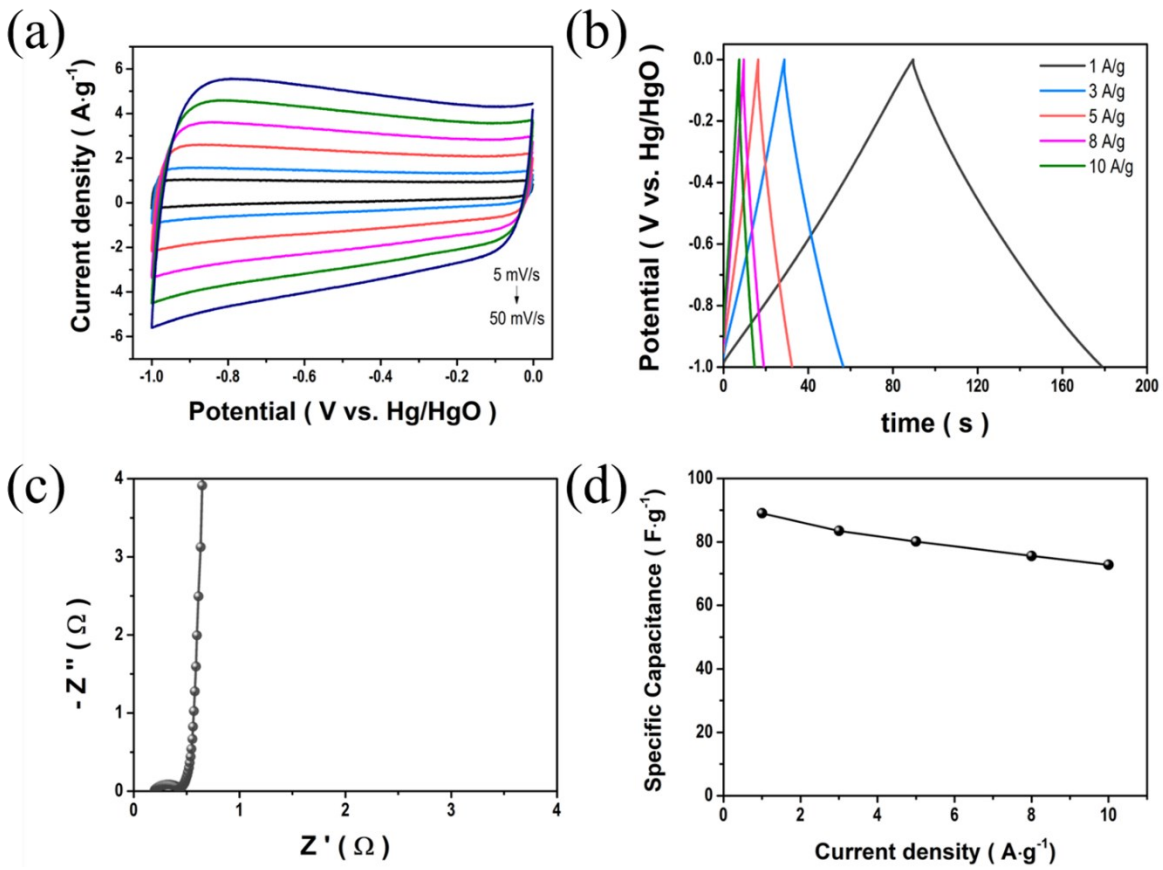

Fig. S8. The electrochemical performances of the AC electrode. (a) CV curves at various scan rates. (b) GCD curves at various current densities. (c) EIS curve. (d) Specific capacitance estimated from GCD curves.

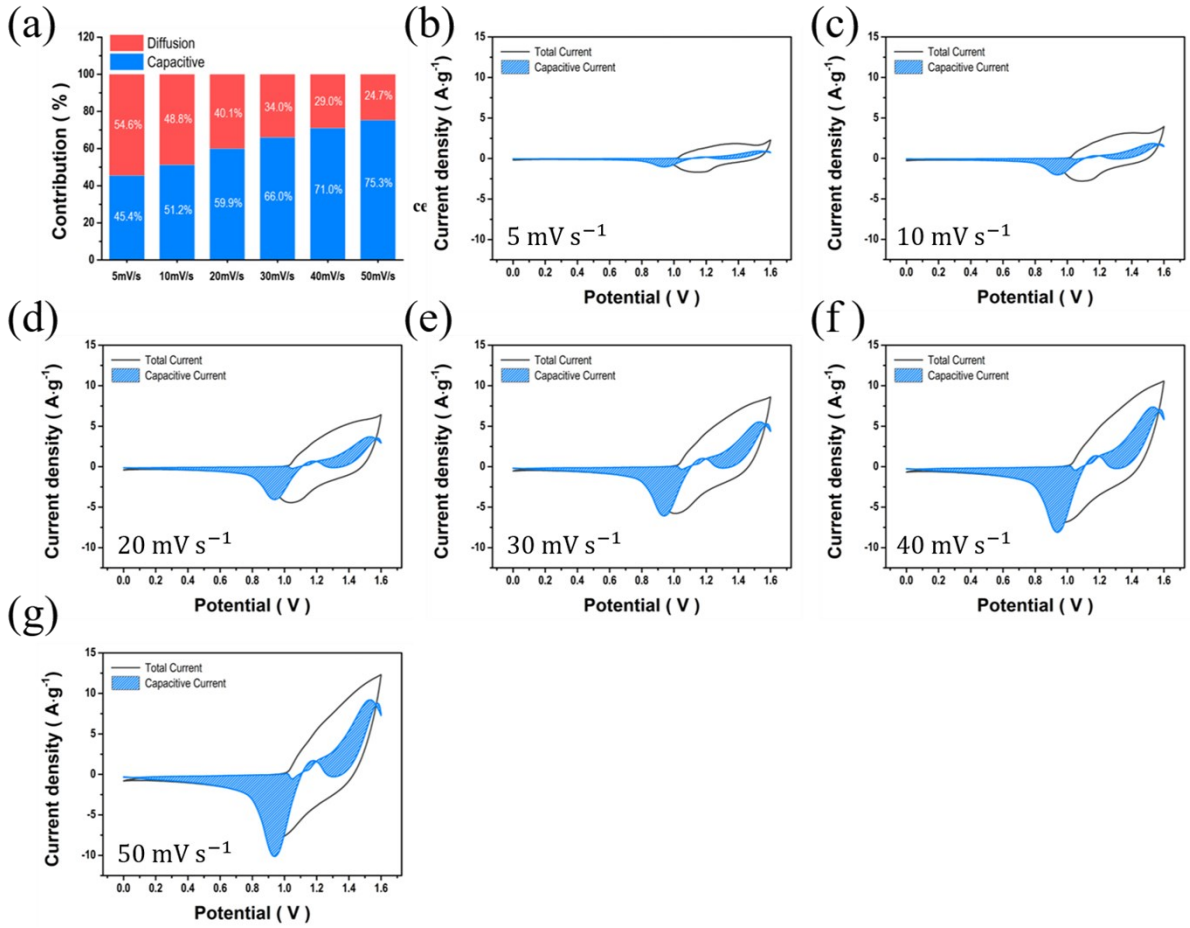

Fig. S9. (a) capacitive and diffusion-controlled contribution of NiCo LDH-$SP_{(1)}$//AC asymmetric device. Comparison of capacitive (blue) and diffusion-controlled (white) contribution schematized in CV curves at (b) 5, (c) 10, (d) 20, (e) 30, (f) 40 and (g) 50 mV s^{-1}.